Determining the selectivity of a tetra-phosphorylated biomimetic peptide towards uranium in the presence of competing cations through the simultaneous coupling of HILIC to ESI-MS and ICP-MS

Lana Abou Zeid, Albert Pell, Marta Garcia Cortes, Hélène Isnard, Pascale Delangle, Carole Bresson

Determining the selectivity of a tetra-phosphorylated biomimetic peptide towards uranium in the presence of competing cations through the simultaneous coupling of HILIC to ESI-MS and ICP-MS

Lana ABOU-ZEID[a, c, #], Albert PELL[a], Marta GARCIA CORTES[a, £], Hélène ISNARD [a], Pascale DELANGLE[b] and Carole BRESSON[a*]

[a] Université Paris-Saclay, CEA, Service de Physico-Chimie F-91191, Gif-sur-Yvette, France

[b] Univ. Grenoble Alpes, CEA, CNRS, GRE-INP, IRIG, SyMMES, 38 000 Grenoble, France

[c] Sorbonne Université, UPMC, F-75005 Paris, France

Current address: Department of Chemistry, Ghent University, Krijgslaan 281-S12, 9000 Ghent, Belgium

£ Current address: Department of Analytical Chemistry, Faculty of Chemistry, Complutense University, Ciudad Universitaria s/n, 28040 Madrid, Spain

* CORRESPONDING AUTHOR: Carole BRESSON

Email address: carole.bresson@cea.fr

KEYWORDS: Uranium, phosphorylated peptide, selectivity, competing ions, HILIC, mass spectrometry/ICP-MS

Abstract

The cyclic tetra-phosphorylated biomimetic peptide (pS1368) has been proposed as a promising starting structure to design decorporating agent of uranyl (UO_2^{2+}) due to its affinity similar to that of osteopontin (OPN), a target UO_2^{2+} protein *in vivo*. The determination of this peptide selectivity towards UO_2^{2+} in the presence of competing endogenous elements is also crucial to validate this hypothesis. In this context, the selectivity of pS1368 towards UO_2^{2+} in the presence of Ca^{2+}, Cu^{2+} and Zn^{2+} was determined by applying the simultaneous coupling of hydrophilic interaction chromatography (HILIC) to electrospray ionization (ESI-MS) and inductively coupled plasma (ICP-MS) mass spectrometry. Sr^{2+} was used as Ca^{2+} simulant, providing less challenging ICP-MS measurements. The separation of the complexes by HILIC were firstly set up. The selectivity of pS1368 towards UO_2^{2+} was determined in the presence of Sr^{2+}, by adding several proportions of this latter to UO_2(pS1368). UO_2^{2+} was not displaced from UO_2(pS1368) even in the presence of a ten-fold excess of Sr^{2+}. The same approach has been undertaken to demonstrate the selectivity of pS1368 towards UO_2^{2+} in the presence of Cu^{2+}, Zn^{2+} and Sr^{2+} as competing endogenous cations. Hence, we showed that pS1368 is selective towards UO_2^{2+} in the presence of Sr^{2+}, but also in the presence of Cu^{2+} and Zn^{2+}. This study highlights the performance of HILIC-ESIMS/ICPMS simultaneous coupling to assess the potential of molecules as decorporating agents of UO_2^{2+}.

1. Introduction

Elements such as Ca, Cu and Zn are essential to humans, as they are mandatory to many biological functions and present in some enzymes and proteins key binding sites [1]. Others such as uranium (U) which is ubiquitous in the earth's crust have no known biological role, making U toxicity of great concern [2]. Indeed, natural U (U_{nat}) exhibits mainly chemical toxicity governed by the interactions of its uranyl (UO_2^{2+}) form with target biomolecules in *vivo* [3]. However, the mechanisms in which UO_2^{2+} is involved at the cellular and molecular levels are still poorly understood. Research is still in progress to characterize the coordination sites of proteins responsible for their affinity towards UO_2^{2+}, which is of prime importance to further develop selective decorporating agents in the event of contamination [4]. To be able to design an efficient decorporating agent, it is essential to determine its selectivity towards the target element in the presence of endogenous ions that are potential competitors [5]. Recently, a tetra-phosphorylated cyclic biomimetic peptide pS1368 (Fig. 1), exhibiting an affinity for UO_2^{2+} similar to that of the hyper-phosphorylated protein osteopontin (OPN), has been proposed as representative of the coordination sites of UO_2^{2+} in this protein [6].

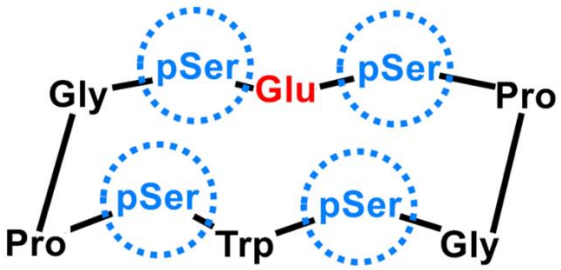

Fig. 1 Structure of the cyclic tetra-phosphorylated peptide pS1368 considered in this work. Adapted from Ref.6.

The selectivity of pS1368 towards UO_2^{2+} in the presence of Ca^{2+}, the cation mainly bound to OPN [7], was deduced by comparing the affinity constants of UO_2(pS1368) and Ca(pS1368). These latter were determined using fluorescence spectroscopy and it was found that the affinity of pS1368 for Ca^{2+} is significantly lower than for UO_2^{2+}, with $K^{pH\ 7.4}$ (Ca(pS1368)) = 10^2, more than nine orders of magnitude lower than $K^{pH\ 7.4}$ (UO_2(pS1368)) = $10^{11.3}$ [6]. These data suggest that pS1368 could be highly selective towards UO_2^{2+} in the presence of physiological amounts of Ca^{2+}. To be able to propose pS1368 as a promising starting structure for UO_2^{2+} decorporation *in vivo*, the determination of its selectivity when

Ca^{2+} and UO_2^{2+} are in a competing complexation reaction is crucial as well as in the presence of other endogenous competing ions, such as Cu^{2+} and Zn^{2+}.

In this work, the methodology that we previously developed [8], based on the simultaneous coupling of HILIC to ESI-MS and ICP-MS, was applied to determine in a single step the selectivity of pS1368 towards UO_2^{2+} in the presence of competing ions at physiological pH. Knowing that OPN binds primarily Ca^{2+} to ensure its biological function [7], this latter cation is the most relevant competing ion for UO_2^{2+} binding to OPN *in vivo*. Therefore, the evaluation of the selectivity of the model peptide pS1368 towards UO_2^{2+} in the presence of Ca^{2+} appears as an essential first step. We chose Sr^{2+} as Ca^{2+} simulant since it has a similar coordination number and ionic radius [9] and exhibits very close physicochemical properties [10], while ensuring less challenging ICP-MS measurements.

The conditions to separate UO_2^{2+} and Sr^{2+} complexes by HILIC [11] were set up. The selectivity of pS1368 towards UO_2^{2+} was then determined in the presence of Sr^{2+} and in a single step, by on-line identifying the separated complexes using ESI-MS and simultaneously quantifying them by ICP-MS [12]. We evaluated then the influence of Sr^{2+} on UO_2^{2+} complexation by pS1368. Through the same approach, we determined the selectivity of pS1368 towards UO_2^{2+} in the presence of Sr^{2+}, Cu^{2+} and Zn^{2+} as competing ions, since they are known to be highly competitive for hard metal cation binding in the blood [13]. To our knowledge, such an analytical approach to assess in a single step the selectivity of a chelating molecule that may be considered as a potential decorporating agent is described for the first time.

2. Experimental part

2.1. Chemicals

Acetonitrile (ACN, CH_3CN, LC-MS grade) and ammonia NH_3 (20-22%) were purchased from VWR prolabo (Briare le canal, France). Ammonium acetate ($NH_4CH_3CO_2$), toluene ($C_6H_5CH_3$, purity > 99.7 %) and ethylenediaminetetraacetic acid (EDTA) tetrasodium salt dihydrate ($Na_4C_{10}H_{12}O_8N_2$, $2H_2O$, 99.5% purity) were supplied by Sigma Aldrich (Saint Quentin Fallavier, France). The cyclic tetra-phosphorylated peptide pS1368 (MW 1291.9 g mol^{-1}) was supplied by Cambridge peptides (Cambridge,

UK) and synthesized following the procedure developed by the CIBEST team [6]. Ultrapure water (18.2 MΩ cm at 25°C) was obtained from Milli-Q purification system (Merck millipore, Guyancourt, France). Certified uranium (U), strontium (Sr), copper (Cu), zinc (Zn), yttrium (Y) and bismuth (Bi) standard solutions (1000 µg mL^{-1} in HNO_3 2% *w/w*), were provided by the SPEX Certiprep Group (Longjumeau, France). L-Tryptophan (L- Trp, 99% purity) was purchased from Acros organics. Nitric acid solutions (HNO_3 2%) were prepared by diluting sub-boiled HNO_3 in ultrapure water. Sub-boiled HNO_3 was prepared by distillating HNO_3 65% (Merck, France) with an evapoclean unit from Analab (France).

2.2. Preparation of stock solutions, contact solutions, samples and standard solutions

2.2.1. ***Stock solutions of uranium, metals and pS1368***

The stock solution of natural uranium (U_{nat}) was obtained by diluting in ultrapure water an in-house U_{nat} solution previously prepared by dissolving uranium oxide powder (U_3O_8) in 0.5 mol L^{-1} HNO_3[14], to achieve a uranium concentration of 10,000 µg mL^{-1} (5 x 10^{-2} mol L^{-1}). The stock solutions of Sr, Cu and Zn were prepared by evaporating to dryness 10 mL of the corresponding SPEX solutions on a hot plate at 95°C, and by recovering the residue with 1 mL of 2% HNO_3 to achieve a metal concentration of 5 x 10^{-2} mol L^{-1}. The concentration of each stock solution was measured by ICP-MS by external calibration using SPEX standard solutions as calibrants.

The pS1368 stock solution was prepared by dissolving 4 mg of the peptide powder in 1 mL of an aqueous solution of $NH_4CH_3CO_2$ (20 mmol L^{-1}, pH ~ 7) to reach a concentration of 3 x 10^{-3} mol L^{-1}. The pS1368 concentration was determined by external calibration using HILIC coupled to UV/VIS in series with ESI-MS, by quantifying the Trp contained in the sequence of the peptide (UV absorption at λ = 280 nm) [8].

2.2.2. ***Contact solutions***

$1UO_2^{2+}:2pS1368:xSr^{2+}$ solutions were obtained by mixing a very small volume of stock solution of U_{nat} (~1.6 µL) with 125 µL of pS1368 stock solution, to reach a UO_2^{2+} concentration of 5x10^{-4} mol L^{-1}.

Different contact solutions of following proportions $1UO_2^{2+}:2pS1368:xSr^{2+}$ (x = 0 to 10) were obtained by addition of 0 - 16 µL of Sr stock solution. The pH was adjusted to 7.4 with NH_3 using a micro-

electrode. All the contact solutions were systematically prepared the day before the analysis and stored at 4°C.

$1UO_2^{2+}$:2pS1368:$1Sr^{2+}$:$1Cu^{2+}$:$1Zn^{2+}$

In a first step, the stability of Cu^{2+}, Zn^{2+} and Sr^{2+} was verified in a solution containing the three elements prepared in 20 mmol L^{-1} of $NH_4CH_3CO_2$. By measuring their concentrations for three consecutive days off-line by ICP-MS, precipitation of Cu^{2+} was observed through the formation of a blue-green precipitate, while this was not the case for Zn^{2+} and Sr^{2+} (See Electronic Supplementary Material Table S1). To overcome this issue, a solution containing Cu^{2+}, Zn^{2+} and Sr^{2+} was prepared in 60 mmol L^{-1} of $NH_4CH_3CO_2$ and the concentration of the metals was monitored for three days by ICP-MS (See Electronic Supplementary Material Table S2). In these conditions, it could be observed that Cu^{2+}, Zn^{2+} and Sr^{2+} were stable under their soluble form. Hence, the contact solution of $1UO_2^{2+}$:2pS1368:$1Sr^{2+}$:$1Cu^{2+}$:$1Zn^{2+}$ was obtained by adding 3 µL of stock solutions of U_{nat}, Sr, Cu and Zn in 250 µL of pS1368 stock solution prepared in $NH_4CH_3CO_2$ 60 mmol L^{-1}, to reach a concentration of $5x10^{-4}$ mol L^{-1} for all elements. The pH was adjusted to 7.4 with NH_3 using a micro-electrode. The contact solution was prepared the day before the analysis and stored at 4°C.

2.2.3. ***Working samples***

The working samples were freshly prepared just before analysis by diluting the contact solutions in the mobile phase made of 72/28 ACN/H_2O *v/v* and 20 mmol L^{-1} $NH_4CH_3CO_2$, to reach a UO_2^{2+} concentration of 10^{-4} mol L^{-1}. The concentration of pS1368 in the working samples was calculated by weight, by considering the stock solution concentration determined by UV/VIS. The total concentration of UO_2^{2+} and metal(s) in the working samples was measured by ICP-MS as described in the section 2.3.

2.2.4. ***Standard solutions***

The standard solutions were prepared in the working mobile phase by mixing in the adequate proportions the U_{nat} stock solution and the Sr SPEX solutions, both at 10 000 µg mL^{-1}, to yield five concentration levels ranging from 6 to 42 µg mL^{-1} for U_{nat} and 6 to 92 µg mL^{-1} for Sr. The tetra-phosphorylated peptide pS1368 was added to the standard solutions in an equimolar ratio with respect to UO_2^{2+} in order to

prevent the hydrolysis of this latter, that is likely to occur in a non-complexing medium [15] but also to obtain specific standard solutions of UO_2^{2+} and Sr^{2+} peptidic complexes [8].

2.3. Selectivity of pS1368 towards UO_2^{2+} in the presence of competing metals

Firstly, the quantification method previously developed using the simultaneous coupling of HILIC-ESIMS/ICPMS [8] was applied to evaluate the selectivity of pS1368 towards UO_2^{2+} in the presence of Sr^{2+}.

The total content of UO_2^{2+} and Sr^{2+}, denoted as $[UO_2^{2+}]_{total}$ and $[Sr^{2+}]_{total}$, were measured in each sample using ICP-MS based on external calibration, by introducing the samples in Flow Injection Analysis (FIA) mode. The samples containing several UO_2^{2+}:2pS1368:xSr^{2+} proportions were injected into the column in duplicate. The Sr^{2+} and UO_2^{2+} complexes were then separated, on-line identified by ESI-MS and the area of the chromatographic peaks obtained by ICP-MS was totally integrated for further quantification of the complexes by the means of external calibration.

The quantitative distribution of UO_2^{2+} and Sr^{2+} among the separated complexes, expressed in percent (%), was calculated as the ratio of the concentration of UO_2^{2+} or Sr^{2+} complexes to the total concentration of these latter in the sample, according to the Equation 1.

$$\% \text{ M(Ligand)} = \frac{[\text{M(Ligand)}]}{[\text{M}]_{total}} \text{ (Equation 1)}$$

With M being UO_2^{2+}or Sr^{2+}.

After each run, around 20% of unbound UO_2^{2+} remained adsorbed on the surface of the stationary phase. Therefore, successive injections of pS1368 were performed to elute this residual fraction.

Secondly, the method was applied to determine the selectivity of pS1368 towards UO_2^{2+} in the presence of competing Cu^{2+}, Zn^{2+} and Sr^{2+} ions. To do this, a model sample containing a mixture of the metals in an equimolar ratio with respect to UO_2^{2+} was considered and denoted $1UO_2^{2+}$:2pS1368:$1Sr^{2+}$:$1Cu^{2+}$:$1Zn^{2+}$.

The sample was introduced in FIA into the ICP-MS to determine the total content of each element through the integration of the total area of the corresponding peaks obtained by recording the signal of the $^{64}Zn^+$, $^{63}Cu^+$, $^{88}Sr^+$, $^{238}U^+$ isotopes. The complexes were further separated, on-line identified by ESI-MS and simultaneously quantified by ICP-MS. Duplicate injections of the sample were performed. The

quantitative distribution of UO_2^{2+} and the metals among the separated complexes, expressed in percent (%), was calculated as the ratio of the peak area of UO_2^{2+} and metal complexes to the peak area of their total elemental content in the sample, according to the Equation 2.

$$\% \text{ M(Ligand)} = \frac{A_{M(Ligand)}}{A_{M\ total}} \text{ (Equation 2)}$$

With M being UO_2^{2+}, Sr^{2+}, Cu^{2+} and A being the peak area.

After each run, successive injections of pS1368 were performed to elute the residual fraction of UO_2^{2+} potentially adsorbed on the surface of the stationary phase.

In all cases, a control sample containing only UO_2^{2+} at 10^{-4} mol L^{-1} and two equivalents of pS1368 was considered.

2.4. Instrumentation

2.4.1. Hydrophilic interaction liquid chromatography

An ultimate 3000 UHPLC$^+$ Dionex/Thermofisher scientific (Courtaboeuf, France) module, made of a degasser, a dual RS pump, an RS autosampler, a column compartment and an RS diode array detector, was used. The metal and UO_2^{2+} complexes were separated using a YMC Triart Diol column (100 x 2 mm; 1.9 µm). Mobile phases of different compositions were obtained by online mixing of solvent A (60/40 ACN/H_2O *v/v* containing 20 mmol L^{-1} $NH_4CH_3CO_2$) and solvent B (80/20 ACN/H_2O *v/v* containing 20 mmol L^{-1} $NH_4CH_3CO_2$) in the adequate proportions. Separations were run in isocratic elution mode at a flow rate of 300 µL min^{-1} and the sample injection volume was 3 µL.

The retention factor *k* of the analytes was calculated following the equation (3):

$$k = \frac{(t_R - t_0)}{t_0} \text{ (Equation 3)}$$

Where t_R is the retention time (min) of the analyte, determined by HILIC-ESI-MS, t_0 is the void time of the toluene as unretained marker (10^{-4} mol L^{-1}, V_{inj} = 1 µL), determined by HILIC-UV/VIS at λ = 254 nm.

The selectivity and resolution factors of the separations, α and R_s respectively, were calculated based on the equations 4 and 5:

$$\alpha = \frac{k_2}{k_1} \text{ (Equation 4)}$$

$$R_s = 1.18 \times \frac{t_{R2} - t_{R1}}{W_{0.5h1} + W_{0.5h2}} \quad \text{(Equation 5)}$$

Being analyte 2 more retained than analyte 1. $W_{0.5}$ corresponds to the full width half-maximum of each peak.

2.4.2. Mass spectrometers

The ESI mass spectrometer was a triple quadrupole TSQ Quantum Ultra™ (Thermo Fisher scientific, San Diego CA, USA) equipped with an H-ESI II ionization probe. All mass spectra were recorded in negative ionization mode by applying the following parameters: spray voltage -3.5 kV, probe temperature 120°C and capillary temperature of 360°C. Direct ESI-MS injection of samples was firstly undertaken in order to identify the most abundant molecular ions. Double charged species of UO_2(pS1368) and free pS1368 were observed, being $[UO_2(pS1368)\text{-}4H]^{2-}$ and $[pS1368\text{-}2H]^{2-}$, in agreement with previous studies [6,8] while mono-charged metal complexes of Sr^{2+} and Cu^{2+} were detected, being $[Sr(CH_3CO_2)_3]^-$ and $[Cu(NO_3)_3]^-$, respectively. For the sake of clarity, the complexes were denoted UO_2(pS1368) and M(ligand) with M = Sr^{2+}, Cu^{2+} along the manuscript, by omitting the charge. Throughout the HILIC-ESI-MS coupling, mass spectra were acquired using full scan (*m/z* 400-1500) and single ion monitoring (SIM) by selecting the *m/z* ratio associated to the most abundant isotope of each species (spectral width: *m/z* ± 0.5, unless stated otherwise), being the free peptide pS1368 and UO_2(pS1368) or metal(ligand) complexes previously determined.

The ICP mass spectrometer was a single quadrupole XSeriesII (Thermo Fisher Scientific). The sample introduction system consisted of a perfluoroalkoxy PFA-ST nebulizer operating at 146.7 µL min^{-1}, and a quartz cyclonic spray chamber thermostated at 3 °C. In order to prevent any carbon deposition due to the use of organic solvents, additional 8 mL min^{-1} oxygen flow rate was introduced in the plasma, through an "additional gas port" located in the spray chamber [16,17]. Furthermore, platinum skimmer, sampler cone and a 1 mm inner diameter injector were used. The tune parameters were daily optimized. Chromatograms were recorded by following the signal of $^{238}U^+$, $^{88}Sr^+$, $^{63}Cu^+$, $^{64}Zn^+$, $^{209}Bi^+$ and $^{89}Y^+$ with an integration time of 90 ms for each isotope, knowing that ^{209}Bi and ^{89}Y were used as internal standards. The simultaneous coupling of HILIC to ESI-MS and ICP-MS was performed according to the setting up described in our previous work [18].

3. Results and discussion

3.1. Definition of HILIC conditions to separate UO_2^{2+} and metal complexes

By applying the chromatographic conditions set up in our previous study [8], a YMC triart diol column and a mobile phase composed of 72/28 ACN/H_2O *v/v* and 20 mmol L^{-1} $NH_4CH_3CO_2$ allowed the successful separation of complexes of UO_2^{2+}, Sr^{2+} and Cu^{2+} following the injection of the model sample $1UO_2^{2+}$:2pS1368:$1Sr^{2+}$:$1Cu^{2+}$:$1Zn^{2+}$. Although the Zn^{2+} complex was not detected by ICP-MS neither by ESI-MS, successive injections of EDTA allowed to recover the whole Zn^{2+} that was adsorbed on the surface of the stationary phase [19]. The chromatograms obtained simultaneously by ESI-MS and ICP-MS are shown in Fig. 2.

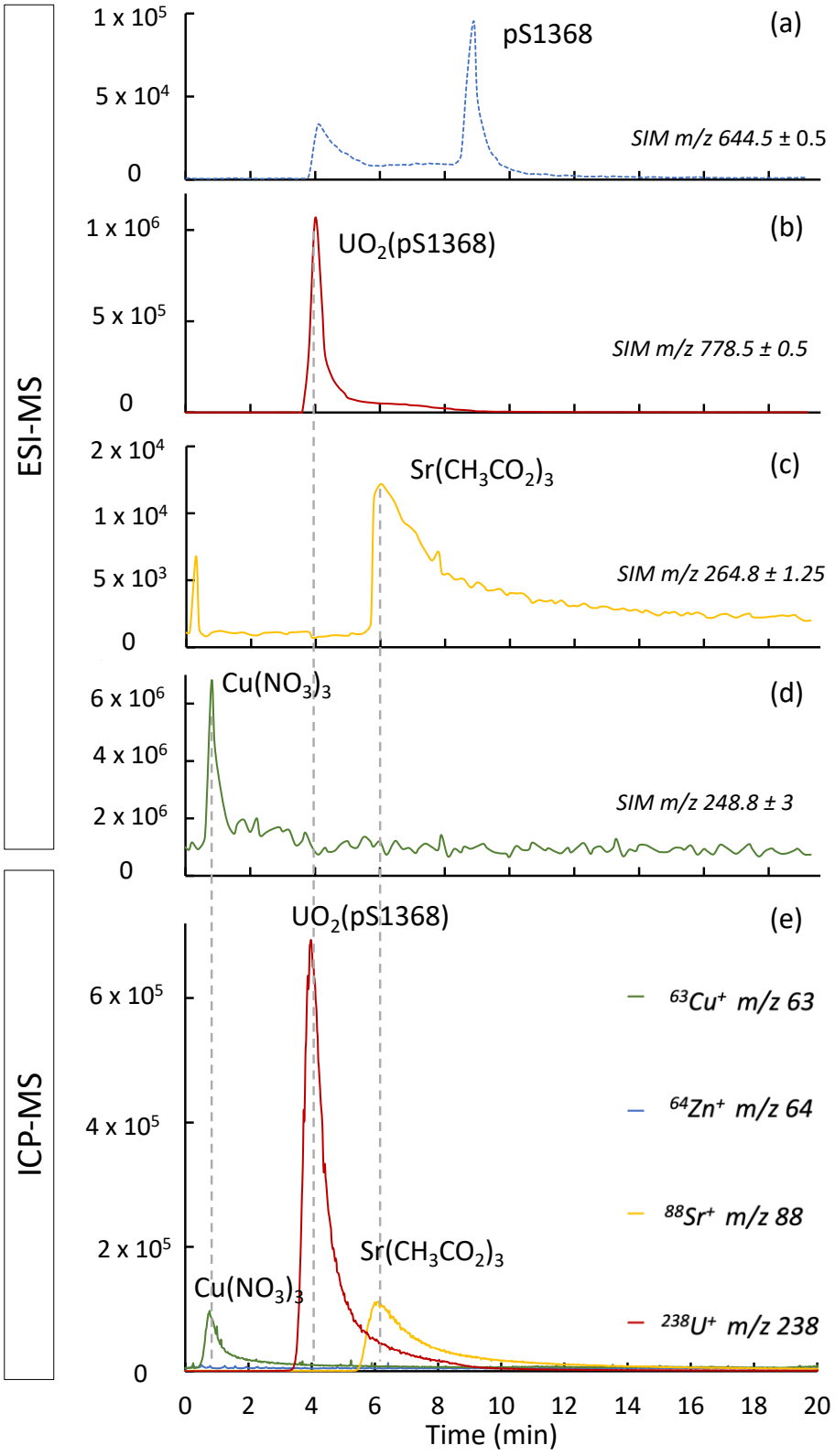

Fig. 2 Separation of UO_2^{2+} and metal complexes by HILIC simultaneously coupled to ESI-MS and ICP-MS. Chromatograms acquired by ESI-MS using SIM mode, centered on the *m/z* ratios of the characteristic ion of pS1368 and considering most abundant isotope of the different elements involved in the complexes (a-d), and (e) superposition of the elution profiles recorded by ICP-MS, following the signal of the most abundant isotopes

$^{238}U^+$, $^{88}Sr^+$, $^{63}Cu^+$ and $^{64}Zn^+$, with an integration time of 90 ms. Sample: $1UO_2{}^{2+}$:2pS1368:$1Sr^{2+}$:$1Cu^{2+}$:$1Zn^{2+}$. Column YMC Triart Diol 100 x 2 mm; 1.9 µm. Mobile phase: 72/28 ACN/H_2O *v/v* with 20 mmol L^{-1} $NH_4CH_3CO_2$, flow rate: 300 µL min^{-1}, V_{inj} = 3µL.

From the elution profiles registered by ICP-MS (Fig 2e), the retention factors of the peaks of $^{63}Cu^+$, $^{238}U^+$ and $^{88}Sr^+$ were 0.5, 4.3 and 6.6, respectively. By comparison of these retention factors with those obtained from the ESI-MS chromatograms (Fig 2b-d), the peaks could be attributed to $Cu(NO_3)_3$, UO_2(pS1368) and $Sr(CH_3CO_2)_3$, respectively. Hence, Sr^{2+} and Cu^{2+} were under the form of acetate or nitrate complexes under these conditions, $UO_2{}^{2+}$ was found as a peptidic complex, while the chemical form of Zn^{2+} could not be identified due to its adsorption on the stationary phase.

3.2. Selectivity of pS1368 towards $UO_2{}^{2+}$ in the presence of Sr^{2+}

Since pS1368 is representative of $UO_2{}^{2+}$ coordination sites in OPN that binds primarily Ca^{2+} to ensure its biological function [7], the evaluation of the selectivity of pS1368 towards $UO_2{}^{2+}$ in the presence of Ca^{2+} is a crucial first step. To meet this aim, several equivalents of Sr^{2+}, used as Ca^{2+} simulant, were added to the UO_2(pS1368) complex at pH 7.4, according to $1UO_2{}^{2+}$:2pS1368:xSr^{2+} ($0 \leq x \leq 10$).

The total $UO_2{}^{2+}$ and Sr^{2+} concentrations in each sample measured by ICP-MS, as well as the targeted and measured $1UO_2{}^{2+}$:2pS1368:xSr^{2+} proportions are listed in table 1.

Table 1: Total $UO_2{}^{2+}$ and Sr^{2+} concentrations measured by ICP-MS using external calibration in samples injected in duplicate and in FIA mode, relative deviation (%) of the values obtained for the two replicates, measured concentration of pS1368, targeted and measured $1UO_2{}^{2+}$:2pS1368:xSr^{2+} proportions.

Targeted $1UO_2{}^{2+}$:2 pS1368: xSr^{2+}	**$[UO_2{}^{2+}]_{total}$** µg mL^{-1} (mol L^{-1})		**Relative deviation (%)**	**[pS1368] mol L^{-1}**	**$[Sr^{2+}]_{total}$** µg mL^{-1} (mol L^{-1})		**Relative deviation (%)**	**Measured $1UO_2{}^{2+}$:2pS1368:xSr^{2+}**
1:2:0	27.3 ($1.1x10^{-4}$)	27.2 ($1.1x10^{-4}$)	0.4	$1.8x10^{-4}$	0.0	0.0	0.0	**1:1.6: 0 (A)**
1:2:1	16.4 ($6.9x10^{-5}$)	16.7 ($7.0x10^{-5}$)	1.3	$1.6x10^{-4}$	5.2 ($5.9x10^{-5}$)	5.3 ($6.0 x10^{-5}$)	1.8	**1:2.4:0.9 (B)**
1:2:2	24.6 ($1.0x10^{-4}$)	24.0 ($1.0x10^{-4}$)	2.2	$2.2x10^{-4}$	16.3 ($1.9 x10^{-4}$)	16.4 ($1.9 x10^{-4}$)	0.2	**1:2.1:1.8 (C)**
1:2:5	23.2 ($9.7x10^{-5}$)	22.1 ($9.3x10^{-5}$)	4.6	$2.0x10^{-4}$	40.6 ($4.6 x10^{-4}$)	40.2 ($4.6 x10^{-4}$)	1.1	**1:2.0:4.7 (D)**
1:2:10	18.6 ($7.8x10^{-5}$)	18.8 ($7.9x10^{-5}$)	1.2	$1.9x10^{-4}$	55.0 ($6.3x10^{-4}$)	54.9 ($6.2 x10^{-4}$)	0.1	**1:2.5:8 (E)**

As can be observed in table 1, the relative deviation between the measured concentrations of $UO_2{}^{2+}$ and Sr^{2+} lies between 0.4 and 4.6% for $UO_2{}^{2+}$ and between 0.1 and 1.8% for Sr^{2+}, showing good repeatability of the measurements.

Following this step, complexes were separated by HILIC, identified online by ESI-MS and simultaneously quantified by ICP-MS following the method described in the experimental part. The separation of the UO_2^{2+} and Sr^{2+} complexes contained in each sample was performed in duplicate, by applying the chromatographic conditions described in part 3.1. The chromatograms simultaneously acquired by ESI-MS and ICP-MS are shown in Fig. 3 for the five samples.

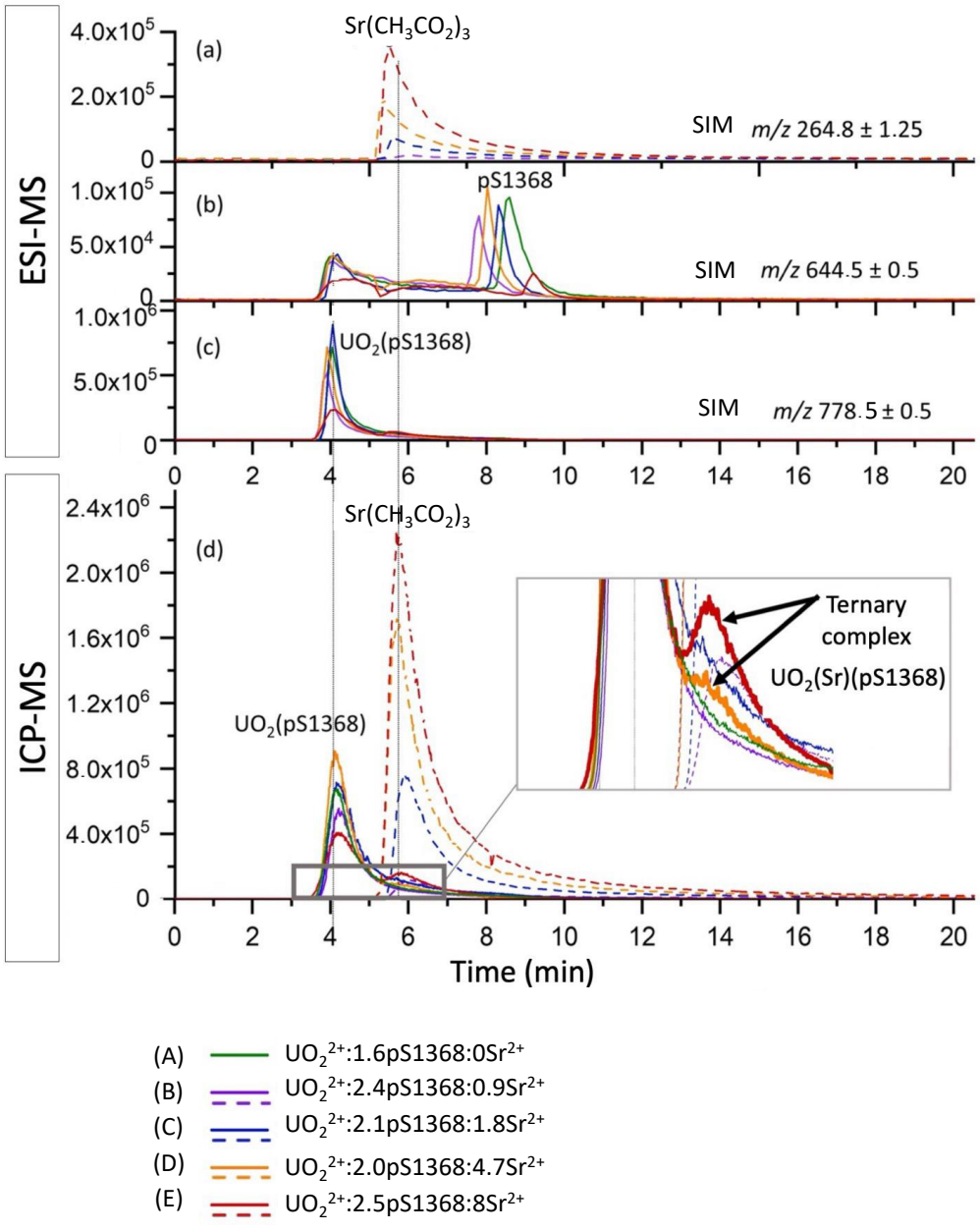

Fig. 3 Separation of UO_2^{2+} and Sr^{2+} complexes by HILIC simultaneously coupled to ESI-MS and ICP-MS. Chromatograms acquired by ESI-MS using SIM mode (a-c), centered on the *m/z* ratios of the characteristic ion of (a) $Sr(CH_3COO)_3$, (b) free pS1368, (c) UO_2(pS1368) considering most abundant isotope of the different elements involved in the complexes and (d) superposition of the elution profiles obtained by ICP-MS, recording

the signal of $^{238}U^{+}$ (solid line) and $^{88}Sr^{+}$ (dotted line) with an integration time of 90 ms. Column YMC Triart Diol 100 x 2 mm; 1.9 µm. Mobile phase: 72/28 ACN/H_2O *v/v* with 20 mmol L^{-1} $NH_4CH_3CO_2$, flow rate 300 µL min^{-1}, V_{inj} = 3µL.

The peaks of $^{238}U^{+}$ and $^{88}Sr^{+}$ obtained by ICP-MS were attributed to UO_2(pS1368) and $Sr(CH_3CO_2)_3$, based on the chromatograms recorded by ESI-MS. No peak corresponding to Sr(pS1368) was observed, showing that Sr^{2+} remains mainly bound to acetate whatever the proportions. In all cases, the chromatographic peak of the free fraction of pS1368 was observed by ESI-MS (Figure 3b). When the number of Sr^{2+} equivalents was equal or higher than 4.7 compared to UO_2^{2+} (samples D and E), a tailing appeared on the UO_2(pS1368) peak registered by ICP-MS, matching with the peak of $Sr(CH_3CO_2)_3$ (Figure 3d). This allowed to suggest the formation of a ternary complex, that can be explained by the ability of pS1368 to coordinate UO_2^{2+} and Sr^{2+} ions through bridging phosphates [6]. In order to check this hypothesis, additional experiments were carried out with the sample E containing the largest amount of Sr^{2+}. This allowed us to identify the ternary complex, owing to the ESI mass spectrum extraction from the tailing peak for acquisitions performed in SIM mode, by applying a mass filter centered on the *m/z* ratio of the ternary complex UO_2(Sr)(pS1368). The chromatograms recorded simultaneously by ESI-MS and ICP-MS are shown in supporting information (See Electronic Supplementary Material Figure S1). Hence, the addition of up to eight equivalents of Sr^{2+} compared to UO_2^{2+} are not sufficient to displace the latter from UO_2(pS1368) and leads instead to the formation of a ternary complex UO_2(Sr)(pS1368). This observation is consistent with literature that reports the formation of ternary complexes of UO_2^{2+}, as $UO_2(Ca)(CO_3)$ [20].

Several attempts have been made to deconvolute the peak of $^{238}U^{+}$ in order to determine the proportion of UO_2^{2+} involved in the ternary complex but did not lead to satisfactory results. Therefore, the quantitative distribution of UO_2^{2+} and Sr^{2+} among the complexes formed in the different samples was determined by applying Equation 1. For D and E samples, the UO_2^{2+} and Sr^{2+} proportions were calculated based on the integration of the chromatographic peak areas including the one involved in the ternary complex, meaning therefore that the quantitative distribution of UO_2^{2+} and Sr^{2+} in the pS1368 complexes was slightly overestimated.

In order to determine the effect of Sr^{2+} addition on the complexation of UO_2^{2+} by pS1368, these values were compared to the proportion of UO_2^{2+} measured in UO_2(pS1368) in the control sample containing $1UO_2^{2+}$:2pS1368, being 79.5 % with respect to total UO_2^{2+} (sample A, Fig. 4).

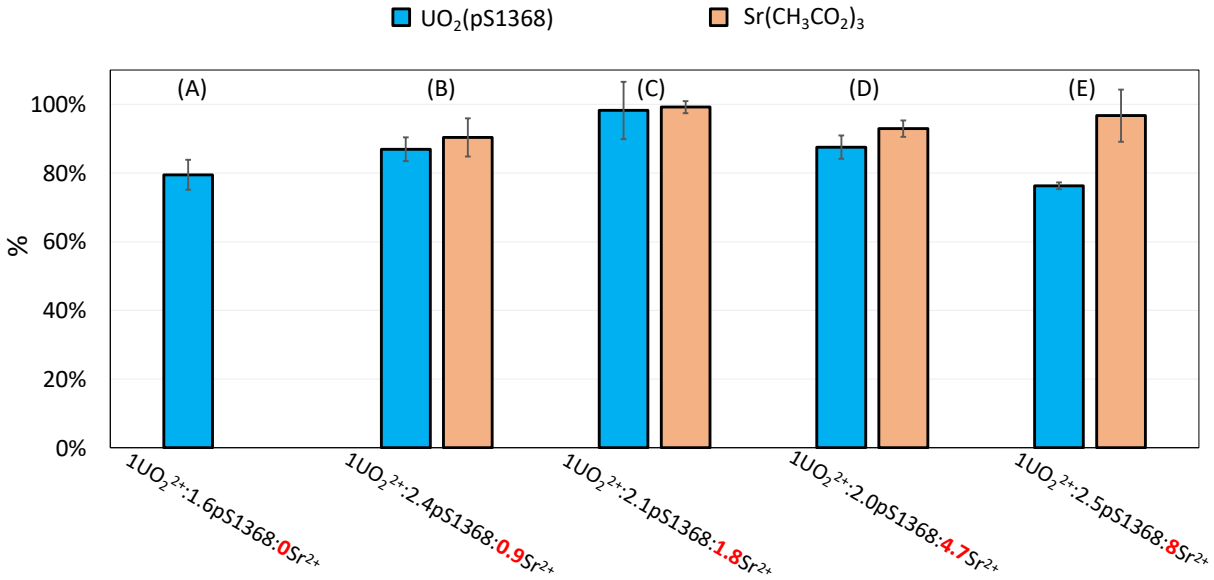

Fig. 4 Proportions of UO_2^{2+} and Sr^{2+} involved in UO_2(pS1368) and $Sr(CH_3CO_2)_3$ complexes for samples (A-E) corresponding to $1UO_2^{2+}$:2pS1368:xSr^{2+}, with x = 0-8. The bars represent the mean value of two measurements of the same sample and the error bars the associated standard deviation.

Regardless the number of Sr^{2+} equivalents, at least 76% of UO_2^{2+} remains bound to pS1368. In addition, more than 90% of Sr^{2+} is in the form of an acetate complex in all the samples. From these results, the selectivity of pS1368 towards UO_2^{2+} was demonstrated even in the presence of an excess of Sr^{2+}, in accordance with the trend observed for the stability constants published previously [6], being $K^{pH\ 7.4}$ (UO_2(pS1368)) = $10^{11.3}$, much higher than $K^{pH7.4}$ (Ca(pS1368)) = 10^2. Hence, the combination of four phosphate binding groups and the cyclic peptide skeleton of pS1368 that orients the latter towards the equatorial plane of UO_2^{2+}, induces efficient selectivity for UO_2^{2+} even in the presence of an excess of Sr^{2+}. Moreover, the low affinity of this peptide for Sr^{2+} as Ca^{2+} analogue, seems to indicate that Ca^{2+} would not bind the phosphorylated pSer residues of OPN, but instead the Aspartate (Asp) and Glutamate (Glu) residues [7]. This is consistent with the larger affinity constants observed for Ca^{2+} with similar model peptides presenting four glutamate/aspartate instead of four phosphoserine residues [21].

3.3. Selectivity of pS1368 towards UO_2^{2+} in the presence of competing cations Cu^{2+}, Zn^{2+} and Sr^{2+}

The selectivity of pS1368 for UO_2^{2+} in the presence of competing cations Cu^{2+}, Zn^{2+} in addition to Sr^{2+} was determined by applying the same approach, using a model sample containing $1UO_2^{2+}$:2pS1368:$1Sr^{2+}$:$1Cu^{2+}$:$1Zn^{2+}$. In the blood, typical concentrations of Ca^{2+}, Cu^{2+} and Zn^{2+} are 2.5 mmol L^{-1}, 50 µmol L^{-1} and 1 µmol L^{-1}, respectively [13]. However, we chose an equimolar ratio of these cations to induce similar competing effects compared to UO_2^{2+}, regarding their complexation ability of pS1368.

The formed complexes were separated using the diol-grafted column and the mobile phase composed of 72/28 ACN/H_2O *v/v* with 20 mmol L^{-1} $NH_4CH_3CO_2$. The quantitative distribution of UO_2^{2+}, Cu^{2+} and Sr^{2+} within the different complexes, determined by ICP-MS as the ratio of the peak area of UO_2^{2+} and metal complexes to the peak of the total elemental content of these latter in the sample, is shown in Fig. 5 for injections in duplicate. Since the Zn^{2+} only eluted owing to successive EDTA injections, the Zn^{2+} quantitative distribution was determined by relating the sum of the areas of the peaks resulting from its column recovery to the peak area of the total Zn^{2+} contained in the sample.

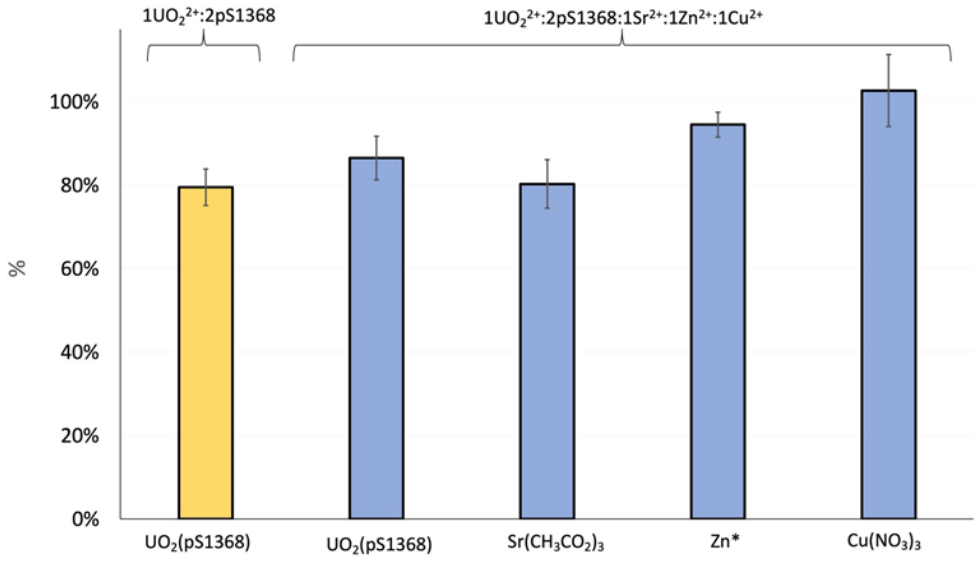

Fig. 5 Proportions of UO_2^{2+}, Sr^{2+} and Cu^{2+} involved in the complexes separated by HILIC. *the complexed proportion was calculated from the recovery of Zn^{2+} adsorbed on the column. The bars represent the mean value of two measurements of the same sample and the error bars represent their standard deviation.

As it can be seen in Fig. 5, more than 80% of UO_2^{2+} is complexed by pS1368 while Sr^{2+} and Cu^{2+} exist mostly (80-100%) as acetate and nitrate complexes, whereas the chemical form of Zn^{2+} could not be identified due to the adsorption of this element on the column. We can also observe that the proportion of UO_2^{2+} involved in UO_2(pS1368) in the model sample is close to the one in the control sample. We can therefore conclude that UO_2^{2+} is not displaced from the UO_2(pS1368) complex by Sr^{2+}, nor by Cu^{2+} or Zn^{2+}, being in equimolar proportions compared to UO_2^{2+}. This shows that pS1368 selectively binds UO_2^{2+} in the presence of these competitors, confirming the interest of this peptide as a selective binding site for the design of decorporating agent of UO_2^{2+} *in vivo*.

4. Conclusion

In this work, a dedicated analytical approach based on the implementation of the simultaneous coupling of HILIC to ESI-MS and ICP-MS was successfully applied to the one-step determination of the selectivity of pS1368 peptide towards UO_2^{2+} in the presence of the competing ions Sr^{2+}, Cu^{2+} and Zn^{2+}. Sr^{2+} was used to mimic the behavior of Ca^{2+} during complexation by pS1368, since it has similar physico-chemical properties, while providing less challenging ICP-MS measurement. The complexes of UO_2^{2+}, Sr^{2+}, Cu^{2+} and Zn^{2+} were separated by HILIC using a YMC triart diol column and a mobile phase composed of 72/28 ACN/H_2O *v/v* with 20 mmol L^{-1} $NH_4CH_3CO_2$, identified online by ESI-MS and simultaneously quantified by ICP-MS. In the presence of increasing number of Sr^{2+} equivalents, more than 76% of UO_2^{2+} remains complexed by pS1368. Furthermore, when the number of Sr^{2+} equivalents compared to UO_2^{2+} is equal or higher than 4.7, a ternary complex UO_2(Sr)(pS1368) is detected. These results led to the conclusion that pS1368 was selective towards UO_2^{2+} in presence of Sr^{2+}, as Ca^{2+} simulant, in agreement with previous results obtained by spectroscopic techniques. The selectivity of this peptide for UO_2^{2+} was also determined in the presence of endogenous competing cations such as Cu^{2+} and Zn^{2+} in addition to Sr^{2+}, all being in equimolar ratio compared to UO_2^{2+}. Under these conditions, UO_2^{2+} is not displaced from UO_2(pS1368). Hence, we demonstrated here that the biomimetic peptide pS1368 is selective for UO_2^{2+} in presence of the three competing endogenous cations Ca^{2+}/Sr^{2+}, Cu^{2+} and Zn^{2+}. The high affinity of the cyclic tetra-phosphorylated peptide pS1368 for UO_2^{2+}

and its selectivity with respect to Sr^{2+} and other endogenous metals thus confirm that pS1368 is an attractive starting scaffold for the design of a selective decorporating agent of UO_2^{2+} *in vivo*.

The method that we developed shows to offer several advantages, in particular the possibility to directly determine the selectivity of pS1368 towards UO_2^{2+} in the presence of endogenous cations, though a competing reaction in the same sample and in one single step. This leads to a reduction of the sample consumption, which is of prime importance for the screening of a large range of chemical or peptide candidates. Overall, these findings highlight the powerful combination of HILIC to ESI-MS and ICP-MS for acquiring in a single step complementary elemental and molecular information which is of prime importance to assess the potential of a candidate molecule as decorporating agent of toxic elements.

Acknowledgements

The authors would like to acknowledge the Cross-Disciplinary Program on Instrumentation and Detection of CEA, the French Alternative Energies and Atomic Energy Commission and the Cross-cutting basic research Program (RTA Program) of the CEA Energy Division, for their financial support.

Declarations

The authors declare that they have no conflicts of interests/competing interests.

5. References

1. Zoroddu MA, Aaseth J, Crisponi G, Medici S, Peana M, Nurchi VM. The essential metals for humans: a brief overview. Journal of Inorganic Biochemistry. 2019;195:120-9.

2. Ma M, Wang R, Xu L, Xu M, Liu S. Emerging health risks and underlying toxicological mechanisms of uranium contamination: Lessons from the past two decades. Environment International. déc 2020;145:106107.

3. Ansoborlo E, Prat O, Moisy P, Den Auwer C, Guilbaud P, Carriere M, et al. Actinide speciation in relation to biological processes. Biochimie. nov 2006;88(11):1605-18.

4. Garai A, Delangle P. Recent advances in uranyl binding in proteins thanks to biomimetic peptides. Journal of Inorganic Biochemistry. févr 2020;203:110936.

5. Ansoborlo É, Amekraz B, Moulin C, Moulin V, Taran F, Bailly T, et al. Review of actinide decorporation with chelating agents. Comptes Rendus Chimie. oct 2007;10(10-11):1010-9.

6. Laporte FA, Lebrun C, Vidaud C, Delangle P. Phosphate-Rich Biomimetic Peptides Shed Light on High-Affinity Hyperphosphorylated Uranyl Binding Sites in Phosphoproteins. Chemistry – A European Journal. 30 mai 2019;25(36):8570-8.

7. Kläning E, Christensen B, Sørensen ES, Vorup-Jensen T, Jensen JK. Osteopontin binds multiple calcium ions with high affinity and independently of phosphorylation status. Bone. sept 2014;66:90-5.

8. Abou-Zeid L, Pell A, Garcia Cortes M, Isnard H, Delangle P, Bresson C. Determination of the affinity of biomimetic peptides for uranium through the simultaneous coupling of HILIC to ESI-MS and ICP-MS. Analytica Chimica Acta. févr 2023;1242:340773.

9. Shannon RD. Revised effective ionic radii and systematic studies of interatomic distances in halides and chalcogenides. Acta Cryst A. 1 sept 1976;32(5):751-67.

10. Raffalt AC, Andersen JET, Christgau S. Application of inductively coupled plasma–mass spectrometry (ICP–MS) and quality assurance to study the incorporation of strontium into bone, bone marrow, and teeth of dogs after one month of treatment with strontium malonate. Anal Bioanal Chem. juill 2008;391(6):2199-207.

11. Nováková L, Havlíková L, Vlčková H. Hydrophilic interaction chromatography of polar and ionizable compounds by UHPLC. TrAC Trends in Analytical Chemistry. déc 2014;63:55-64.

12. Bresson C, Ansoborlo E, Vidaud C. Radionuclide speciation: A key point in the field of nuclear toxicology studies. J Anal At Spectrom. 2011;26(3):593.

13. Cacheris WP, Quay SC, Rocklage SM. The relationship between thermodynamics and the toxicity of gadolinium complexes. Magnetic Resonance Imaging. janv 1990;8(4):467-81.

14. Paredes E, Avazeri E, Malard V, Vidaud C, Reiller PE, Ortega R, et al. Evidence of isotopic fractionation of natural uranium in cultured human cells. Proc Natl Acad Sci USA. 6 déc 2016;113(49):14007-12.

15. Sutton M, Burastero SR. Uranium(VI) Solubility and Speciation in Simulated Elemental Human Biological Fluids. Chem Res Toxicol. nov 2004;17(11):1468-80.

16. Leclercq A, Nonell A, Todolí Torró JL, Bresson C, Vio L, Vercouter T, et al. Introduction of

organic/hydro-organic matrices in inductively coupled plasma optical emission spectrometry and mass spectrometry: A tutorial review. Part I. Theoretical considerations. Analytica Chimica Acta. juill 2015;885:33-56.

17. Leclercq A, Nonell A, Todolí Torró JL, Bresson C, Vio L, Vercouter T, et al. Introduction of organic/hydro-organic matrices in inductively coupled plasma optical emission spectrometry and mass spectrometry: A tutorial review. Part II. Practical considerations. Analytica Chimica Acta. juill 2015;885:57-91.

18. Blanchard E, Nonell A, Chartier F, Rincel A, Bresson C. Evaluation of superficially and fully porous particles for HILIC separation of lanthanide–polyaminocarboxylic species and simultaneous coupling to ESIMS and ICPMS. RSC Adv. 2018;8(44):24760-72.

19. Xuan Y, Scheuermann EB, Meda AR, Hayen H, von Wiren N, Weber G. Separation and identification of phytosiderophores and their metal complexes in plants by zwitterionic hydrophilic interaction liquid chromatography coupled to electrospray ionization mass spectrometry. JOURNAL OF CHROMATOGRAPHY A. 8 déc 2006;1136(1):73-81.

20. Kelly SD, Kemner KM, Brooks SC. X-ray absorption spectroscopy identifies calcium-uranyl-carbonate complexes at environmental concentrations. Geochimica et Cosmochimica Acta. févr 2007;71(4):821-34.

21. Lebrun C, Starck M, Gathu V, Chenavier Y, Delangle P. Engineering Short Peptide Sequences for Uranyl Binding. Chem Eur J. 8 déc 2014;20(50):16566-73.

7. Figure captions

Fig. 1 Structure of the cyclic tetra-phosphorylated peptide pS1368 considered in this work. Adapted from Ref.6.

Fig. 2 Separation of UO_2^{2+} and metal complexes by HILIC simultaneously coupled to ESI-MS and ICP-MS. Chromatograms acquired by ESI-MS using SIM mode, centered on the *m/z* ratios of the characteristic ion of pS1368 and considering most abundant isotope of the different elements involved in the complexes (a-d), and (e) superposition of the elution profiles recorded by ICP-MS, following the signal of the most abundant isotopes $^{238}U^+$, $^{88}Sr^+$, $^{63}Cu^+$ and $^{64}Zn^+$, with an integration time of 90 ms. Sample: $1UO_2^{2+}$:2pS1368:$1Sr^{2+}$:$1Cu^{2+}$:$1Zn^{2+}$. Column YMC Triart Diol 100 x 2 mm; 1.9 µm. Mobile phase: 72/28 ACN/H_2O *v/v* with 20 mmol L^{-1} $NH_4CH_3CO_2$, flow rate: 300 µL min^{-1}, V_{inj} = 3µL.

Fig. 3 Separation of UO_2^{2+} and Sr^{2+} complexes by HILIC simultaneously coupled to ESI-MS and ICP-MS. Chromatograms acquired by ESI-MS using SIM mode (a-c), centered on the *m/z* ratios of the characteristic ion of (a) $Sr(CH_3COO)_3$, (b) free pS1368, (c) UO_2(pS1368) considering most abundant isotope of the different elements involved in the complexes and (d) superposition of the elution profiles obtained by ICP-MS, recording the signal of $^{238}U^+$ (solid line) and $^{88}Sr^+$ (dotted line) with an integration time of 90 ms. Column YMC Triart Diol 100 x 2 mm; 1.9 µm. Mobile phase: 72/28 ACN/H_2O *v/v* with 20 mmol L^{-1} $NH_4CH_3CO_2$, flow rate 300 µL min^{-1}, V_{inj} = 3µL.

Fig. 4 Proportions of UO_2^{2+} and Sr^{2+} involved in UO_2(pS1368) and $Sr(CH_3CO_2)$ complexes for samples (A-E) corresponding to $1UO_2^{2+}$:2pS1368:xSr^{2+}, with x = 0-8. The bars represent the mean value of two measurements of the same sample and the error bars the associated standard deviation.

Fig. 5 Proportions of UO_2^{2+}, Sr^{2+} and Cu^{2+} involved in the complexes separated by HILIC. *the complexed proportion was calculated from the recovery of Zn^{2+} adsorbed on the column. The bars represent the mean value of two measurements of the same sample and the error bars represent their standard deviation.